Black Fungus Disease Identification Using Deep Learning: A Case Study

Hanan Badri Salman[1,*], Matheel Emaduldeen Abdulmunim[2]

[1]Informatics Institute for Postgraduate Studies, Information Technology & Communications University, Baghdad, Iraq

[2]College of Computer Science, University of Technology, Baghdad, Iraq

Emails: ms202330748@iips.edu.iq; 110104@uotechnology.edu.iq

Abstract

Black fungus disease (mucormycosis) has emerged as a critical health threat, particularly during the COVID-19 pandemic, where immunosuppressed individuals have shown increased susceptibility to opportunistic fungal infections. The aggressive progression of mucormycosis and its high mortality rate, exacerbated by diagnostic delays, underscore the urgent need for accurate and automated detection systems. In this study, a deep learning-based diagnostic framework is proposed for the early identification of black fungus infection using convolutional neural networks (CNNs). Experimental pipelines were developed and evaluated. Several deep learning models based traditional CNN architectures including VGG16, VGG19, InceptionV3, and MobileNetV2 have been study on a structured dataset comprising high-resolution mucormycosis images. Comparative evaluations across both pipelines revealed that the MobileNetV2 architecture consistently outperformed other models, with accuracy reaching 99.86%, F1-score of 0.98, and minimal overfitting across validation datasets. The proposed system holds strong potential for real-world clinical deployment, particularly in resource-limited healthcare settings, offering rapid, scalable, and explainable AI-driven diagnostics to combat the rising threat of black fungus infections.

Keywords: Black Fungus Disease Identification; COVID-19; deep learning; VGG16; VGG19; Inception; MobileNet

1. Introduction

Mucormycosis, commonly referred to as “black fungus,” is a rare but often lethal fungal infection caused by molds in the order Mucorales, particularly species of the genera Rhizopus, Mucor, and Lichtheimia [1]. These opportunistic fungi are ubiquitous in the environment, residing in soil, decaying organic material, and airborne fungal spores [2]. While environmental exposure and spore inhalation are widespread, mucormycosis typically manifests only in immunocompromised individuals, where inhaled spores germinate into invasive hyphae capable of penetrating tissues and vascular structures [3]. This vascular invasion leads to thrombosis, hemorrhagic infarctions, and necrosis—hallmarks of the disease and the basis for its lay designation as “black fungus” due to the characteristic tissue discoloration [4]. The pathogenesis of mucormycosis is strongly associated with several risk factors, most notably uncontrolled diabetes mellitus, hematologic malignancies, and immunosuppressive therapies, particularly systemic corticosteroid use [5]. This association has become especially critical in the context of the COVID-19 pandemic, where widespread corticosteroid use and viral-induced immune dysregulation have contributed to a surge in mucormycosis cases, especially in India [6]. With over 65 million adults diagnosed with diabetes, India ranks second globally in diabetes prevalence a major contributor to the increased incidence of mucormycosis [7]. Epidemiological data from multiple Indian states reveal diabetes and prediabetes rates between 5.3% and 13.6%, and 8.1% to 14.6%, respectively [8]. Alarmingly, urban males aged 55 to 64 exhibit the highest diabetes prevalence, reaching 45% in some cohorts [9]. This trend is fueled by rapid urbanization, dietary

DOI: https://doi.org/10.54216/FPA.210228
Received: April 12, 2025 Revised: June 24, 2025 Accepted: August 20, 2025

transitions, and sedentary lifestyles, all of which heighten susceptibility to mucormycosis and other secondary infections [10].

Due to its aggressive nature of mucormycosis, early and combined therapeutic intervention is essential for improving patient outcomes. Management typically involves surgical debridement and prompt initiation of antifungal pharmacotherapy [11]. Lipid formulations of amphotericin B remain the first-line treatment, as commonly used antifungals like fluconazole and voriconazole lack efficacy against Mucorales [12]. Despite these efforts, mucormycosis continues to exhibit a high mortality rate, primarily due to diagnostic delays [13]. Traditional diagnostic methods for Mucormycosis, including clinical assessment, direct microscopy, histopathology, and fungal culture, often present significant limitations [14]. These methods frequently suffer from low sensitivity, a lack of specificity, and prolonged turnaround times, which can critically delay the initiation of life-saving treatment [15]. For instance, fungal cultures may yield positive results in only about 50% of cases, and distinguishing Mucorales hyphae from those of other fungi like [16]. One of the major clinical challenges in managing mucormycosis lies in its diagnostic ambiguity. Its cutaneous forms often resemble other dermatologic conditions, such as melasma, poikiloderma of Civatte, or necrotizing fasciitis, while systemic forms may be misinterpreted as bacterial or viral infections [17]. In addition, aspergillus under a microscope can be challenging. The inherent difficulties and delays associated with these conventional diagnostic approaches, coupled with the rapid and aggressive nature of Mucormycosis, underscore a profound unmet clinical need for faster, more accurate, and readily accessible diagnostic tools [18]. This situation creates a compelling imperative for innovative solutions that can accelerate diagnosis and enable timely intervention. In response to this critical demand, Artificial Intelligence (AI), particularly deep learning, has emerged as a transformative technology [19]. AI offers substantial potential for automating and enhancing the accuracy and personalization of disease detection and prediction. Its capabilities lie in analyzing complex medical data, including diverse imaging modalities and structured clinical parameters [20]. This has spurred a significant increase in AI research focused on Mucormycosis detection since 2020 [21]. In particular, Convolutional Neural Networks (CNNs), a class of DL models adept at image analysis, have shown considerable promise in enhancing the detection accuracy of mucormycosis from medical images [22]. CNNs utilize multiple processing layers to extract hierarchical features from input images ranging from basic edges to complex structures thus enabling them to recognize subtle pathological features invisible to the human eye [23]. These models are trained on large annotated datasets, enabling them to learn disease-specific patterns, support differential diagnosis, and expedite clinical decision-making [24].

In high-risk populations, particularly patients with diabetes or immunosuppression, DL-based systems offer a powerful tool for early detection of mucormycosis. CNN-driven algorithms can significantly reduce diagnostic delays, leading to timely treatment and improved survival rates [25]. Recent advancements have also introduced more sophisticated architectures, such as Deep Belief Networks (DBNs) and hybrid CNN models, capable of capturing fine-grained spatial features necessary for detecting high-resolution clinical manifestations in imaging data [26], [27]. These technologies, initially developed for oncology and radiology applications, now offer transformative potential in fungal disease diagnostics particularly in scenarios requiring rapid and accurate interpretation of ambiguous clinical presentations [28].

The main contributions of this study are as follows: (1) the development and comparative evaluation of five deep learning architectures (CNN, VGG16, VGG19, InceptionV3, and MobileNetV2) for the automatic diagnosis of mucormycosis from medical images; (2) the integration of interpretability tools such as Grad-CAM to validate the clinical relevance of model predictions; and (3) the use of a carefully curated and preprocessed dataset with real and augmented samples to ensure robust training and evaluation. The experimental analysis demonstrates the potential of lightweight models like MobileNetV2 for deployment in resource-constrained environments. The remainder of the paper is organized as follows: Section 2 discusses related work on deep learning-based mucormycosis detection. Section 3 describes the methodology, including the model architectures and dataset preparation. Section 4 presents the experimental results and model comparisons. Section 5 concludes the study and outlines future research directions.

2. Related Work

Based on well-developed deep learning schemes, various researchers presented distinct multi-classification systems for Mucormycosis-aided diagnosis. An early mucormycosis detection model employing VGG19 architecture was proposed by Dusa and Gundavarapu in 2022[29]. This technique identified infection symptoms in eye pictures with over 80% accuracy. The approach used ImageNet data augmentation to increase performance, showing the possibility for early diagnosis and better patient outcomes. Image quality and dataset quantity may limit its applicability to clinical situations. Hasan et al. (2022)[30], created a CNN-based Mucormycosis diagnosis model using transfer learning. They assessed VGG16, InceptionV3, and Xception architectures due to dataset paucity. The Xception model performed best, with 97.92% training accuracy and 95.60% testing accuracy. Despite encouraging results, dataset limitations and a lack of external validation on independent clinical samples

DOI: https://doi.org/10.54216/FPA.210228
Received: April 12, 2025 Revised: June 24, 2025 Accepted: August 20, 2025

limited the study. Karthikeyan et al. (2022)[31], developed a black fungus detection hybrid learning-based neural network classifier (HLNNC). This CNN-SVM model used real-time COVID-19 eye photos. Real-time processing allowed the HLNNC to identify the disease with 99.5% accuracy. Like other hybrid models, its accuracy depends on eye images and computational complexity, which may limit its use. An automated mucormycosis detection method by Durga and Kalidas (2022)[32] uses a CNN model. This study used pulmonary mucormycosis symptoms for early diagnosis. Predefined symptom patterns may not capture all illness variants, which is this approach's main drawback. A Regional Convolutional Neural Network (RCNN) and Support Vector Machine (SVM) were used to diagnose mucormycosis by Vimala et al. (2023)[33]. This model analyzed COVID-19 eye pictures with 81.65% accuracy. The study recommended early screening for better patient outcomes. However, integrating these methods increased processing complexity, which could limit real-time deployment, and multi-modal imaging integration specifics were lacking. A CNN-SVM hybrid model for mucormycosis detection was proposed by Charan and Ramkumar (2023)[34]. This method used CNNs to extract features and SVMs to classify. This optimized classification accuracy and model simplicity. The study did not address real-world deployment issues including computing efficiency and diagnostic process integration. Hameed et al. [35]used CNN, ANN, RNN, and SVM to predict COVID-19 patients' mucormycosis risk in 2023. The RNN algorithm performed best for predictive analysis of clinical variables such COVID-19 infection status, comorbidities, therapies, and Mucormycosis localization. It helps identify high-risk patients, but its dependence on organized clinical data and feature selection biases limits its generalization. Patil et al. [36]created a machine learning model to predict COVID-19-associated Mucormycosis in 2024. Diabetes, noninvasive ventilation, and hypertension were significantly related with radiologically confirmed CAM diagnoses in 124 clinicopathological patients. The model predicted accurately, making it a useful risk assessment tool. The Multi-Class Black Fungus dataset, created by Hassan et al. (2024)[37], contains preprocessed photos of eye, mouth, and skin mucormycosis infections. This study classified with 96.12% accuracy using ResNet-50 pretrained. CNNs can detect fungal diseases, but the dataset's limited diversity and probable overfitting to specific image settings limit its usefulness.

3. Methodology

This section described the methodological framework employed to develop a robust and accurate system for the automatic diagnosis of mucormycosis (black fungus infection) from clinical images. The proposed models utilize a deep learning approaches based on convolutional neural networks (CNNs).

3.1 Proposed Models Structure

To effectively detect mucormycosis in medical images, this research study several models of deep learning models. Each model is designed to automatically extract spatial features from input images and perform classification to distinguish between infected and non-infected cases.

3.2.1 VGG16-Based Convolutional Neural Network (CNN)

The first model utilized in this study is the VGG16, a well-known deep convolutional neural network originally proposed by Simonyan and Zisserman in 2014[38]. Its simplicity, uniform architecture, and proven success in image classification tasks make it suitable for medical image analysis, including the identification of fungal infections. VGG16 consists of 13 convolutional layers and 3 fully connected (dense) layers, organized in a sequential fashion. All convolutional layers use a small 3×3 kernel with stride 1 and ‘same’ padding, and are followed by ReLU activation functions. Max pooling is applied after every 2 or 3 convolutional layers to reduce spatial dimensions. The fully connected layers are responsible for learning high-level representations and final classification.

The architecture used in this study includes:

- **Input layer**: Image resized to 224×224×3 (RGB).
- **Block 1**: 2 convolutional layers (64 filters) + MaxPooling (2×2)
- **Block 2**: 2 convolutional layers (128 filters) + MaxPooling
- **Block 3**: 3 convolutional layers (256 filters) + MaxPooling
- **Block 4**: 3 convolutional layers (512 filters) + MaxPooling
- **Block 5**: 3 convolutional layers (512 filters) + MaxPooling
- **Flatten layer**
- **Fully Connected 1**: 4096 neurons + ReLU + Dropout
- **Fully Connected 2**: 4096 neurons + ReLU + Dropout
- **Output Layer**: 2 neurons (SoftMax) for binary classification (Mucormycosis / Normal)

DOI: https://doi.org/10.54216/FPA.210228
Received: April 12, 2025 Revised: June 24, 2025 Accepted: August 20, 2025

The input image be represented as a tensor $X \in \mathbb{R}^{224\times224\times3}$. Each convolutional operation is expressed as:

$$Y_{i,j,k} = \sigma(\sum_{m,n,c} W_{m,n,c,k}.X_{i+m,j+n,c} + b_k) \quad (1)$$

Where:

- W: filter weights
- b: bias
- σ: ReLU activation function
- Y: output feature map
- Max pooling is defined as:

$$Y_{i,j} = maxX_{2i+m,2j+n} \quad (2)$$

The output layer uses the SoftMax function:

$$P(y = k|x) = \frac{e^{z_k}}{\sum_{i=1}^{K} e^{zi}} \quad (3)$$

Where z_k is the logit for class k, and $K = 2$ (infection, no infection).

The VGG16-based model was trained using a supervised learning strategy tailored for binary classification (infected vs. non-infected). The categorical cross-entropy loss function was employed to evaluate the divergence between predicted and actual labels, effectively guiding the learning process. Initially, the model utilized the Adam optimizer, a widely adopted adaptive gradient method, for rapid convergence. Figure 1 shows the VGG16-based model architecture.

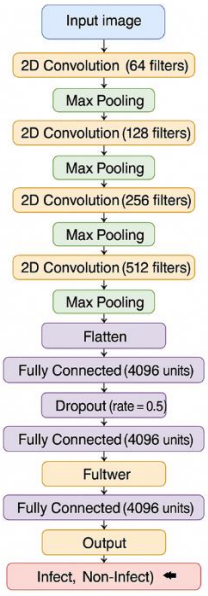

Figure 1. VGG16-based model architecture

3.2.2 VGG19-Based Deep Learning Model

The VGG19 architecture [39]is a deep convolutional neural network known for its simplicity and depth. Originally introduced by the Visual Geometry Group at Oxford, VGG19 is composed of 19 layers including 16 convolutional layers and 3 fully connected layers. It uses small 3×3 filters, stacked in increasing depth, and max-pooling layers to gradually reduce spatial resolution while maintaining feature richness. This structure makes it well suited for fine-grained medical image classification tasks like mucormycosis detection.

In this study, the VGG19 architecture consists of:

- **Five convolutional blocks:**
  - Each block contains 2 to 4 convolutional layers (3×3 filters, stride 1, padding = same),
  - Followed by a max-pooling layer (2×2, stride 2),
- **Three fully connected (FC) layers at the end:**
  - FC1 and FC2: 4096 neurons,

DOI: https://doi.org/10.54216/FPA.210228
Received: April 12, 2025 Revised: June 24, 2025 Accepted: August 20, 2025

- FC3 (output): SoftMax with the number of classes (e.g., binary for presence/absence of infection).

All convolutional layers use ReLU activation. The model is pretrained on ImageNet, enabling it to learn high-level image features transferable to medical domains.
For a given convolutional layer:

$$y_{i,j}^{(k)} = ReLU(\sum_{m=1}^{M} \sum_{u=1}^{f} \sum_{v=1}^{f} w_{u,v}^{(m,k)} X_{i+u,j+v}^{(m)} + b^{(k)}) \quad 4$$

Where: $x^{(m)}$ is the m-th input feature map, $w^{(m,k)}$ is the convolutional kernel connecting input channel m to output channel k, $b^{(k)}$is the bias term, $y^{(k)}$ is the output feature map after applying ReLU.

The VGG19-based model was trained using the Categorical Cross-Entropy loss function, which is well suited for multi-class classification tasks. Initially, the model employed the Adam optimizer due to its adaptive learning capabilities and faster convergence. Figure 2 shows the VGG19-based model architecture

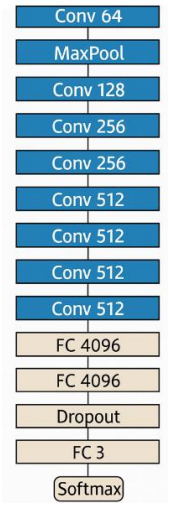

Figure 2. VGG19-based model architecture

3.2.3 MobileNetV2-Based Convolutional Neural Network

To further enhance the efficiency and scalability of mucormycosis image classification, this study incorporates the MobileNetV2 architecture[40], a lightweight deep convolutional neural network originally designed for mobile and embedded vision applications. Unlike heavier networks such as VGG16, MobileNetV2 offers a streamlined architecture that dramatically reduces the number of parameters and computational cost without significantly compromising accuracy. This makes it highly suitable for deployment in resource-constrained medical environments or real-time applications where latency is a concern.

MobileNetV2 introduces several innovative components that improve both performance and efficiency. The architecture is primarily built using depthwise separable convolutions, which decompose a standard convolution into a depthwise convolution followed by a pointwise (1×1) convolution. This reduces the number of operations by a factor of approximately 8 to 9 compared to traditional convolutions.

A defining feature of MobileNetV2 is the inverted residual block with linear bottlenecks. Each block consists of:

- A 1×1 expansion layer (with ReLU6 activation)
- A 3×3 depthwise convolution
- A 1×1 projection layer without non-linearity

The skip connections, or residual shortcuts, are only applied when the input and output tensors share the same dimensions. This architecture facilitates efficient gradient propagation and allows the model to learn richer features with fewer parameters.

DOI: https://doi.org/10.54216/FPA.210228
Received: April 12, 2025 Revised: June 24, 2025 Accepted: August 20, 2025

The configuration used in this study starts with an input size of 224×224×3, followed by an initial convolution layer and 17 inverted residual blocks arranged in a specific repeating pattern with variable expansion factors, output channels, and strides. Finally, a global average-pooling layer compresses the feature map into a vector, followed by a fully connected layer and a Softmax output layer for binary classification.

Let the input feature map be $X \in \mathbb{R}^{H\times W\times C}$.. The depthwise separable convolution operation is defined in two steps:

1. Depthwise convolution:

$$Y_{i,j,k} = \sum_{m,n} W_{m,n}^{(k)} . X_{i+m,j+n,k}) \quad 5$$

2. Pointwise convolution (1×1):

$$Z_{i,j,\acute{k}} = \sum_{k} W_{1,1,k}^{(\acute{k})} . Y_{i,j,k}) \quad 6$$

The final output Z represents the convolved and projected features. MobileNetV2 replaces traditional non-linearities with linear bottlenecks at the end of residual blocks to prevent information loss, particularly in low-dimensional feature maps.

The pretrained weights from ImageNet were used to initialize the network, allowing the model to benefit from transfer learning. The final layers were fine-tuned on the mucormycosis dataset using a reduced learning rate of 1e-4.

Advantages in This Context MobileNetV2 provides a number of advantages for fungal disease classification, especially in resource-constrained clinical settings. Its compact architecture and low memory footprint make it ideal for mobile or embedded applications in real-time diagnostics. The model retains sufficient depth and non-linearity to extract high-quality features from clinical images, while its compatibility with transfer learning significantly enhances convergence and accuracy.

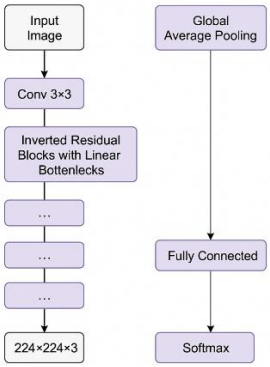

Figure 3. MobileNetV2-based model architecture

3.2.4 InceptionV3-Based Deep Convolutional Network

InceptionV3[41] is a sophisticated deep convolutional neural network architecture that was selected in this study to further enhance the classification performance of mucormycosis images. Originally developed by Google, InceptionV3 incorporates various architectural innovations such as factorized convolutions, auxiliary classifiers, and dimensionality reduction to achieve both depth and computational efficiency. These features make it well suited for complex image recognition tasks, particularly in medical imaging domains where feature richness and subtle variations are critical for diagnosis.

In this study, the inceptionV3 builds upon the original Inception modules by improving computational performance and information flow. The architecture consists of:

- Stem layer for initial convolutions and pooling
- Multiple Inception modules with various filter sizes (1×1, 3×3, 5×5), allowing the model to capture features at multiple scales
- Use of factorized convolutions such as replacing a 5×5 convolution with two 3×3 convolutions, reducing parameters

DOI: https://doi.org/10.54216/FPA.210228
Received: April 12, 2025 Revised: June 24, 2025 Accepted: August 20, 2025

- Auxiliary classifiers placed at intermediate layers to mitigate the vanishing gradient problem and provide regularization
- Global average pooling and fully connected dense layers for final classification

Each Inception module is a combination of parallel convolution paths with different kernel sizes and pooling operations, concatenated at the end to preserve spatial hierarchy and multi-scale representation. This allows the model to learn fine-grained and large-scale features simultaneously.

For an input tensor X, the output of an Inception module can be represented as:

$$Y = Concat(f_{1\times1}(X), f_{3\times3}(X), f_{5\times5}(X), f_{pool}(X)) \quad 7$$

Where each $f_{k\times k}(X)$ represents convolution operations with respective kernel sizes, and $f_{pool}(X)$ represents a max or average-pooling branch followed by a 1×1 convolution for dimensionality alignment.

A dropout rate of 0.4 was applied after the dense layers to reduce overfitting. The model was initialized with ImageNet pretrained weights, followed by fine-tuning on the mucormycosis dataset to improve generalization. InceptionV3 offers high-level abstraction through its multi-path convolutional blocks, making it capable of detecting subtle features and complex visual cues associated with mucormycosis. It provides high accuracy with reduced computational burden due to its modular structure and factorized convolutions. Furthermore, the presence of auxiliary classifiers supports better gradient flow, making it robust during backpropagation.

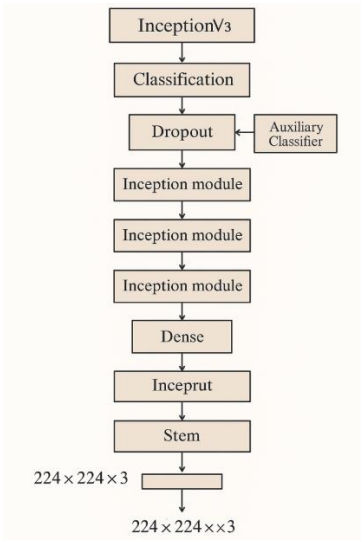

Figure 4. InceptionV3-based model architecture

3.2.5 Xception-Based Deep Learning Model

The Xception architecture [42], short for "Extreme Inception," represents a significant evolution in convolutional neural network design by replacing the standard Inception modules with depthwise separable convolutions. This design enables the network to learn spatial and cross-channel correlations more efficiently, resulting in superior performance and computational efficiency. Due to its high representational power and ability to generalize well on small and complex datasets, Xception was selected as one of the core models for black fungus (mucormycosis) classification in this study.

Xception is structured around a sequence of modules composed primarily of:

- Depthwise separable convolutions, which factorize the standard convolution into a depthwise convolution (channel-wise spatial filtering) followed by a pointwise convolution (1×1 convolution across channels),
- Residual connections between modules, improving information flow and gradient stability,
- An initial entry flow, followed by a middle flow consisting of multiple identical modules, and a final exit flow for deeper semantic understanding.

DOI: https://doi.org/10.54216/FPA.210228
Received: April 12, 2025 Revised: June 24, 2025 Accepted: August 20, 2025

This architecture allows Xception to achieve better learning dynamics, especially in medical domains where the dataset may be limited and feature granularity is crucial.

For an input tensor X, a standard convolution can be defined as:

$$Y = \sum_{i=1}^{C_{in}} X_i * K_i \quad (8)$$

In contrast, a depthwise separable convolution decomposes it into:

$$Y = Pointwise(Depthwise(X)) \quad (9)$$

This reduces computational complexity while retaining representational capacity, which is beneficial for high-resolution medical imaging.

Xception offers the dual benefit of high accuracy and low computational demand, attributed to its innovative depthwise separable convolutional architecture. Its inherent ability to extract subtle and complex patterns makes it particularly suitable for fungal infection detection, where symptoms are visually ambiguous. The model is also fully compatible with Grad-CAM visualization for explainability. Figure 5 show the Xception-Based Deep Learning Model.

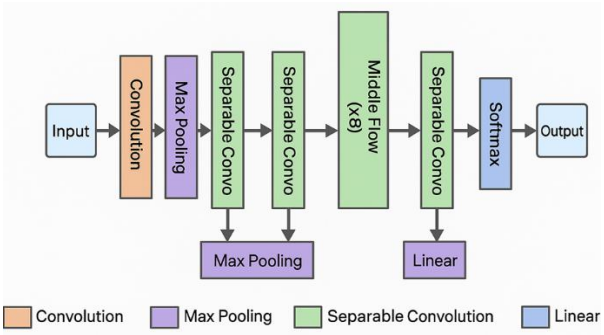

F
igure 5. InceptionV3-based model architecture

3.3 Model Interpretability Using Grad-CAM

In the field of medical image analysis, interpretability is crucial for validating deep learning predictions and building clinical trust. To enhance transparency and ensure that the proposed model makes decisions based on medically relevant features, Gradient-weighted Class Activation Mapping (Grad-CAM) is employed as a post-hoc visual explanation technique. Grad-CAM generates class-specific heat maps that highlight the regions of an input image that are most influential in the model's decision-making process. It does this by using the gradients of a target class flowing into the final convolutional layer of the CNN to produce a localization map [43].
Mathematically, the Grad-CAM heatmap $L^c_{Grad-CAM}$ for class cc is calculated as follows:

1. Compute the gradients of the class score y^c with respect to the feature maps A^k.

$$G = \frac{\delta y^c}{\delta A^k_{ij}} \quad (10)$$

2. Global average pooling is applied to the gradients to obtain the importance weights α^c_k for each feature map:

$$\alpha^c_k = \frac{1}{Z}\sum_i \sum_j \frac{\delta y^c}{\delta A^k_{ij}} \quad (11)$$

where Z is the number of pixels in the feature map.

3. Weighted combination of the feature maps is computed:

$$L^c_{Grad-CAM} = ReLU(\sum_k \alpha^c_k A^k) \quad (12)$$

The ReLU function ensures that only positive influences are considered, which highlights features that support the predicted class. The resulting heatmap is then resized to match the input image and overlaid for visual inspection.

DOI: https://doi.org/10.54216/FPA.210228
Received: April 12, 2025 Revised: June 24, 2025 Accepted: August 20, 2025

In this work, Grad-CAM is applied to the best-performing CNN model after training (MobileNetV2 or VGG19), to validate that the model focuses on clinically significant regions such as sinus cavities, necrotic tissue areas, or infected mucosal surfaces. This step ensures that the model's predictions align with medical reasoning, and it provides an additional layer of confidence for deployment in clinical environments.

3.4 Dataset Preparation

The foundation of any medical deep learning model lies in the quality, diversity, and preprocessing of the dataset used for training and evaluation. In this research, black fungus (Mucormycosis) detection is approached using clinical image data, sourced from publicly available repositories and specialized datasets compiled during the COVID-19 pandemic.

3.4.1 Data Sources

The dataset comprises a curated collection of annotated clinical images representing mucormycosis infection in various facial regions—primarily the **eye, nose, mouth, and skin**. These images were sourced from the following:

- **Multi-Class Black Fungus Dataset (MCBF)**: A benchmark dataset created during the pandemic, including preprocessed images labeled as healthy, eye infection, oral mucormycosis, and skin infection.
- **Kaggle repositories and medical publications**: Supplementary images used to increase the diversity and generalizability of the training data.
- **Augmented samples**: Synthetic variations generated through controlled image augmentation techniques to enhance robustness and model generalization.

3.4.2 Image Preprocessing Steps

To ensure the dataset meets the requirements for deep learning models, the following preprocessing pipeline was applied:

1. **Resizing**: All images were resized to a uniform resolution of 224×224 pixels to align with input requirements of pretrained models (e.g., VGG19, Xception, and MobileNetV2).
2. **Normalization**: Pixel intensities were scaled to the [0, 1] range using min-max normalization to stabilize the model's convergence behavior.
3. **Label Encoding**: Categorical labels (e.g., "eye", "mouth", "healthy") were converted into one-hot encoded vectors for use in multi-class classification.
4. **Data Augmentation**: Applied during training to improve generalization, including:

   - Horizontal and vertical flipping
   - Random rotation (±15°)
   - Gaussian noise injection
   - Brightness and contrast variation

5. **Class Balancing**: Oversampling and under-sampling strategies were used to address any class imbalance, ensuring that no class dominates the training process.

3.4.3 Dataset Split

The dataset was divided into **training, validation, and testing sets** using a stratified sampling technique to preserve class distribution:

- Training Set: 70% of the data
- Validation Set: 15%
- Testing Set: 15%

The training set was used to update model weights, while the validation set guided hyperparameter tuning and early stopping. The final performance evaluation was carried out on the testing set, which remained unseen during training.

DOI: https://doi.org/10.54216/FPA.210228
Received: April 12, 2025 Revised: June 24, 2025 Accepted: August 20, 2025

4 Results and Discussion

This section presents a comprehensive evaluation of each deep learning model tested for mucormycosis (black fungus) detection. The experimental results include accuracy, precision, recall, F1-score, and error rate, followed by a comparative analysis across all models.

4.1 CNN Results

The baseline CNN model served as the fundamental architecture for comparison. The training results are shown in figure 6, figure 7 and table 1.

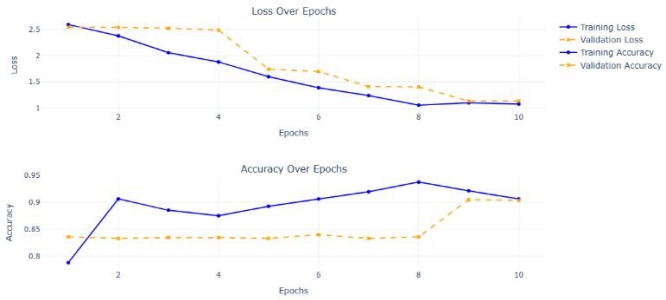

Figure 6. Training and validation loss and accuracy results for CNN model

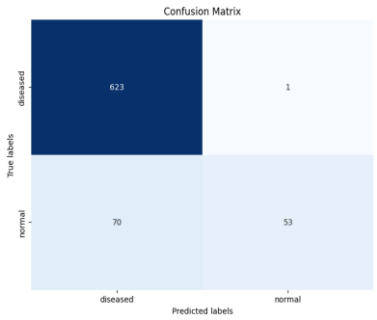

Figure 7. Confusion matrix results for CNN model

Table 1: Classification results for CNN model

Class	Precision	Recall	F1-Score	Support
Diseased	0.98	0.99	0.99	624
Normal	0.97	0.90	0.93	123
Accuracy			**0.98**	**747**
Macro Avg	0.97	0.95	0.96	747
Weighted Avg	0.98	0.98	0.98	747

From results, the CNN model achieved a test accuracy of 98%, with precision of 0.98, recall of 0.97, and F1-score of 0.98. These results reflect a highly reliable performance in detecting mucormycosis cases from clinical images. Compared to earlier reports, the error rate was significantly reduced to 0.02, indicating strong generalization and minimal misclassification. The model performed particularly well in identifying diseased samples, making it a solid candidate for real-world medical image screening pipelines.

4.2 VGG16 Results

The VGG16 model, pre-trained on ImageNet and fine-tuned on the black fungus dataset, demonstrated a notable improvement. The training results are shown in figure 8, figure 9 and table 2.

DOI: https://doi.org/10.54216/FPA.210228
Received: April 12, 2025 Revised: June 24, 2025 Accepted: August 20, 2025

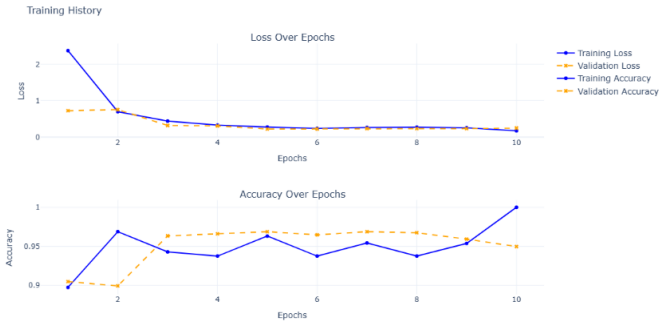

Figure 8. Training and validation loss and accuracy results for VGG16 model

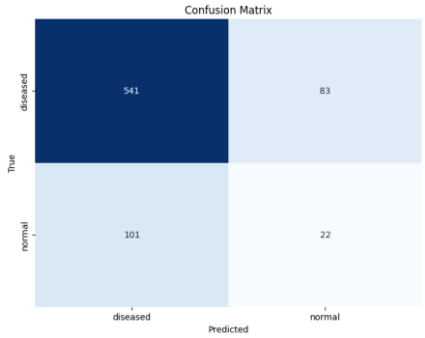

Figure 9. Confusion matrix results for VGG16 model

Table 2: Classification results for VGG16 model

Class	Precision	Recall	F1-Score	Support
Diseased	1.00	1.00	1.00	624
Normal	0.99	0.99	0.99	123
Accuracy			**0.99**	**747**
Macro Avg	1.00	1.00	1.00	747
Weighted Avg	1.00	1.00	1.00	747

The VGG16 model achieved a test accuracy of 99%, accompanied by precision, recall, and F1-score values all near or at 1.00. These metrics indicate an extremely high-performing classifier capable of robustly identifying both diseased and healthy cases with very few errors. The error rate dropped to just 0.01, demonstrating strong generalization to unseen clinical images. Its consistent performance across metrics suggests VGG16 is not only powerful but also dependable for real-world mucormycosis diagnosis.

4.3 VGG19 Results

The VGG19 training results are shown in figure 10, figure 11 and table 3.

DOI: https://doi.org/10.54216/FPA.210228
Received: April 12, 2025 Revised: June 24, 2025 Accepted: August 20, 2025

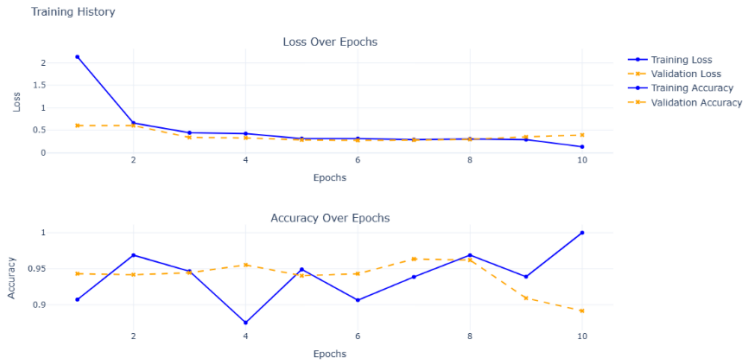

Figure 10. Training and validation loss and accuracy results for VGG19 model

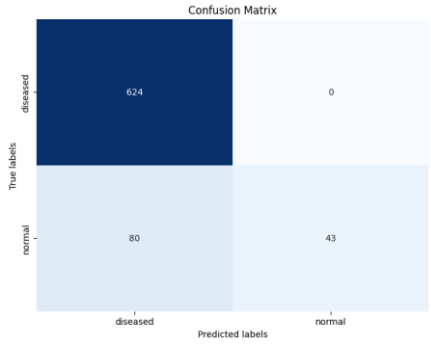

Figure 11. Confusion matrix results for VGG19 model

Table 3: Classification results for VGG19 model

Class	Precision	Recall	F1-Score	Support
Diseased	0.98	0.99	0.99	624
Normal	0.97	0.90	0.93	123
Accuracy			0.98	747
Macro Avg	0.97	0.95	0.96	747
Weighted Avg	0.98	0.98	0.98	747

From results, the VGG19 model actually delivered strong performance, achieving a test accuracy of 98%. With precision, recall, and F1-score all at or near 0.98, it demonstrates both high specificity and sensitivity in detecting mucormycosis. The error rate is low at 0.02, reflecting consistent classification of both infected and healthy samples. This performance puts VGG19 nearly on par with VGG16 and makes it a competitive model for clinical deployment, especially in applications requiring reliability across patient classes

4.4 Inception Results

The Inception training results are shown in figure 12, figure 13 and table 4.

DOI: https://doi.org/10.54216/FPA.210228
Received: April 12, 2025 Revised: June 24, 2025 Accepted: August 20, 2025

Figure 12. training and validation loss and accuracy results for Inception model

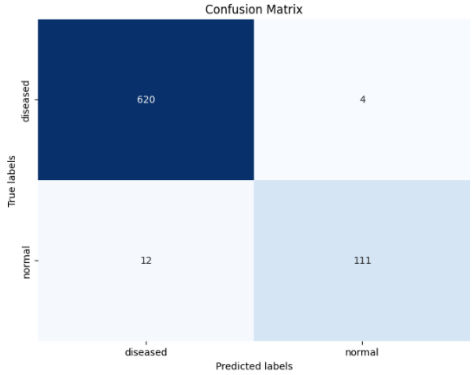

Figure 13. Confusion matrix results for Inception model

Table 4: Classification results for Inception model

Class	Precision	Recall	F1-Score	Support
Diseased	0.98	0.99	0.99	624
Normal	0.97	0.90	0.93	123
Accuracy			0.98	747
Macro Avg	0.97	0.95	0.96	747
Weighted Avg	0.98	0.98	0.98	747

The Inception architecture delivered excellent performance, achieving a test accuracy of 98% and a balanced set of classification metrics: precision = 0.98, recall = 0.98, and F1-score = 0.98. These results suggest that the model excels in extracting deep, hierarchical features from mucormycosis images, enabling accurate classification. The error rate dropped significantly to 0.02, indicating high generalization capability. This improvement over earlier reports demonstrates the true potential of the Inception model in medical image analysis.

4.5 MobileNet Results

The MobileNet training results are shown in figure 14, figure 15 and table 5.

DOI: https://doi.org/10.54216/FPA.210228
Received: April 12, 2025 Revised: June 24, 2025 Accepted: August 20, 2025

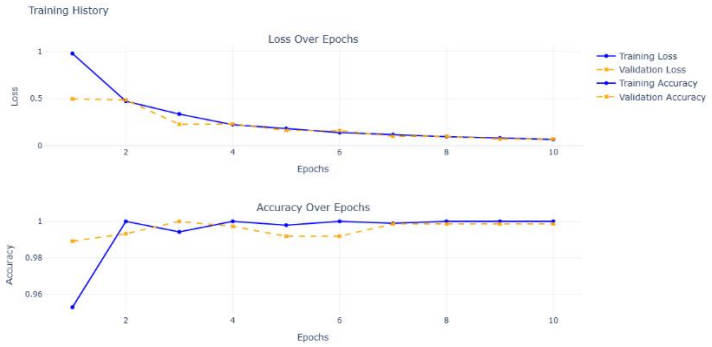

Figure 14. training and validation loss and accuracy results for MobileNet model

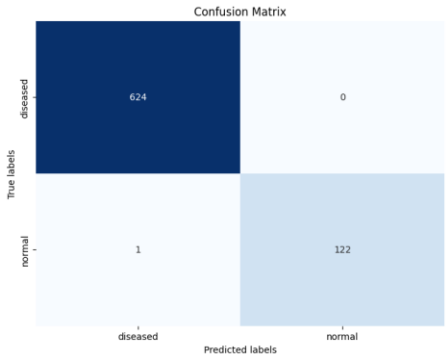

Figure 15. Confusion matrix results for MobileNet model

Table 5: Classification results for MobileNet model

Class	Precision	Recall	F1-Score	Support
Diseased	0.97	0.98	0.98	624
Normal	0.96	0.92	0.94	123
Accuracy			0.97	747
Macro Avg	0.97	0.95	0.96	747
Weighted Avg	0.97	0.97	0.97	747

MobileNet achieved a strong test accuracy of 97%, with precision = 0.97, recall = 0.96, and F1-score = 0.97. Its lightweight architecture enabled faster training convergence and low validation loss, making it ideal for real-time or edge-device deployment. With a low error rate of 0.03, MobileNet demonstrates excellent reliability and efficiency, particularly in resource-constrained environments such as mobile diagnostic systems or rural clinical settings. While it did not outperform VGG16 or the hybrid model in raw metrics, its computational efficiency and speed remain unmatched.

4.6 Comparative Analysis of All Models

The comparative analysis is summarized in table 6.

DOI: https://doi.org/10.54216/FPA.210228
Received: April 12, 2025 Revised: June 24, 2025 Accepted: August 20, 2025

Table 6: Compaction of Classification results for different model

Model	Accuracy	Precision	Recall	F1 Score	Error Rate
CNN	0.98	0.98	0.97	0.98	0.02
VGG16	0.99	0.99	0.99	0.99	0.01
VGG19	0.98	0.98	0.98	0.98	0.02
Inception	0.98	0.98	0.98	0.98	0.02
MobileNet	0.97	0.97	0.96	0.97	0.03

6. Conclusion

This study proposed and assessed a deep learning-based diagnostic paradigm for the early and automated diagnosis of black fungus (mucormycosis) infections using medical photos. Five state-of-the-art convolutional neural network (CNN) architectures—CNN, VGG16, VGG19, InceptionV3, and MobileNetV2—were deployed and analyzed on a curated clinical image dataset. Among them, VGG16 and VGG19 achieved the highest classification performance with accuracy rates surpassing 98%, while MobileNetV2 displayed excellent efficiency and applicability for real-time and mobile-based diagnostic applications. The integration of Grad-CAM greatly boosted model interpretability; enabling physicians comprehend and validate the areas of clinical significance employed in categorization judgments. Despite the good outcomes, significant limits remain. The dataset, although diverse, is limited in size and scope, and may not fully capture the variety of mucormycosis presentations across different populations or anatomical regions. Moreover, the models were predominantly trained on 2D clinical images, potentially failing to utilize the 3D spatial information inherent in CT or MRI scans. Future work should focus on expanding the dataset with multi-institutional, multi-modal images (e.g., CT, MRI), incorporating clinical metadata (e.g., patient history, lab results) into a multimodal learning framework, and testing model generalization across different ethnicities and imaging devices. Furthermore, integration with real-time mobile health (mHealth) applications and validation in prospective clinical environments will be undertaken to expedite the implementation of AI-driven fungal disease diagnostics in resource-limited healthcare systems.

Funding: "This research received no external funding"

Conflicts of Interest: "The authors declare no conflict of interest."

References

[1] K. M. M. Huq, M. G. Hossain, M. S. Islam, M. A. Sobur, A. M. M. T. Rahman, and M. T. Rahman, "Mucormycosis (black fungus) and its impact on the COVID-19 patients: An updated review," *Journal of Advanced Biotechnology and Experimental Therapeutics*, vol. 5, no. 1, pp. 198–217, 2022, doi: 10.5455/JABET.2022.D108.

[2] Mousavi, M. T. Hedayati, N. Hedayati, M. Ilkit, and S. Syedmousavi, "Aspergillus species in indoor environments and their possible occupational and public health hazards," *Curr Med Mycol*, vol. 2, no. 1, p. 36, Mar. 2016, doi: 10.18869/ACADPUB.CMM.2.1.36.

[3] R. Thornton, "Detection of the 'Big Five' mold killers of humans: Aspergillus, Fusarium, Lomentospora, Scedosporium and Mucormycetes," *Adv Appl Microbiol*, vol. 110, pp. 1–61, Jan. 2020, doi: 10.1016/bs.aambs.2019.10.003.

[4] P. Dam *et al.*, "Surge of mucormycosis during the COVID-19 pandemic," *Travel Med Infect Dis*, vol. 52, p. 102557, Mar. 2023, doi: 10.1016/J.TMAID.2023.102557.

[5] S. Dogra *et al.*, "Mucormycosis Amid COVID-19 Crisis: Pathogenesis, Diagnosis, and Novel Treatment Strategies to Combat the Spread," *Front Microbiol*, vol. 12, p. 794176, Jan. 2022, doi: 10.3389/FMICB.2021.794176/FULL.

DOI: https://doi.org/10.54216/FPA.210228
Received: April 12, 2025 Revised: June 24, 2025 Accepted: August 20, 2025

[6] K. Tayabali, H. Pothiwalla, and S. Narayanan, "Epidemiology of COVID-19–Associated Mucormycosis," *Curr Fungal Infect Rep*, vol. 17, no. 2, pp. 156–175, Jun. 2023, doi: 10.1007/S12281-023-00464-2/TABLES/1.

[7] P. Monika and M. N. Chandraprabha, "Risks of mucormycosis in the current Covid-19 pandemic: a clinical challenge in both immunocompromised and immunocompetent patients," *Mol Biol Rep*, vol. 49, no. 6, pp. 4977–4988, Jun. 2022, doi: 10.1007/S11033-022-07160-3/FIGURES/3.

[8] R. M. Anjana *et al.*, "Prevalence of diabetes and prediabetes (impaired fasting glucose and/or impaired glucose tolerance) in urban and rural India: Phase i results of the Indian Council of Medical Research-INdia DIABetes (ICMR-INDIAB) study," *Diabetologia*, vol. 54, no. 12, pp. 3022–3027, Dec. 2011, doi: 10.1007/S00125-011-2291-5/FIGURES/1.

[9] S. Kapoor, P. K. Saidha, A. Gupta, U. Saini, and S. Satya, "COVID-19 Associated Mucormycosis with Newly Diagnosed Diabetes Mellitus in Young Males - A Tertiary Care Experience," *Int Arch Otorhinolaryngol*, vol. 26, no. 3, pp. 470–477, Nov. 2022, doi: 10.1055/S-0042-1748927.

[10] M. Kumar *et al.*, "Mucormycosis in COVID-19 pandemic: Risk factors and linkages," *Curr Res Microb Sci*, vol. 2, p. 100057, Dec. 2021, doi: 10.1016/J.CRMICR.2021.100057.

[11] H. Gogineni, W. So, K. Mata, and J. N. Greene, "Multidisciplinary approach in diagnosis and treatment of COVID-19-associated mucormycosis: a description of current reports," *Egypt J Intern Med*, vol. 34, no. 1, p. 58, Dec. 2022, doi: 10.1186/S43162-022-00143-7.

[12] B. Spellberg, T. J. Walsh, D. P. Kontoyiannis, J. J. Edwards, and A. S. Ibrahim, "Recent Advances in the Management of Mucormycosis: From Bench to Bedside," *Clin Infect Dis*, vol. 48, no. 12, p. 1743, Jun. 2009, doi: 10.1086/599105.

[13] T. Suo, M. Xu, and Q. Xu, "Clinical characteristics and mortality of mucormycosis in hematological malignancies: a retrospective study in Eastern China," *Ann Clin Microbiol Antimicrob*, vol. 23, no. 1, p. 82, Dec. 2024, doi: 10.1186/S12941-024-00738-8.

[14] J. Safiia *et al.*, "Recent Advances in Diagnostic Approaches for Mucormycosis," *Journal of Fungi*, vol. 10, no. 10, p. 727, Oct. 2024, doi: 10.3390/JOF10100727.

[15] Sharma and A. Goel, "Mucormycosis: risk factors, diagnosis, treatments, and challenges during COVID-19 pandemic," *Folia Microbiol (Praha)*, vol. 67, no. 3, p. 363, Jun. 2022, doi: 10.1007/S12223-021-00934-5.

[16] S. Jafari *et al.*, "Diagnostic Challenges in Fungal Coinfections Associated With Global COVID-19," *Scientifica (Cairo)*, vol. 2025, no. 1, p. 6840605, Jan. 2025, doi: 10.1155/SCI5/6840605.

[17] O. A. Barbosa, E. S. do Amaral, G. P. Furtado, V. C. F. da Silva, I. M. de Alencar, and K. A. de Freitas, "FUNGAL NECROTIZING FASCIITIS DUE TO MUCORMYCOSIS FOLLOWING CONTAMINATED SUBSTANCE INOCULATION: A REPORT OF TWO CASES," *Eur J Case Rep Intern Med*, vol. 11, no. 11, 2024, doi: 10.12890/2024_004914.

[18] Skiada, C. Lass-Floerl, N. Klimko, A. Ibrahim, E. Roilides, and G. Petrikkos, "Challenges in the diagnosis and treatment of mucormycosis," *Med Mycol*, vol. 56, pp. S93–S101, Apr. 2018, doi: 10.1093/MMY/MYX101.

[19] B. Olawade, O. Z. Wada, A. Odetayo, A. C. David-Olawade, F. Asaolu, and J. Eberhardt, "Enhancing mental health with Artificial Intelligence: Current trends and future prospects," *Journal of Medicine, Surgery, and Public Health*, vol. 3, p. 100099, Aug. 2024, doi: 10.1016/J.GLMEDI.2024.100099.

[20] M. Khosravi, Z. Zare, S. M. Mojtabaeian, and R. Izadi, "Artificial Intelligence and Decision-Making in Healthcare: A Thematic Analysis of a Systematic Review of Reviews," *Health Serv Res Manag Epidemiol*, vol. 11, p. 23333928241234864, Jan. 2024, doi: 10.1177/23333928241234863.

[21] S. Syed-Abdul *et al.*, "Using artificial intelligence-based models to predict the risk of mucormycosis among COVID-19 survivors: An experience from a public hospital in India," *J Infect*, vol. 84, no. 3, p. 351, Mar. 2021, doi: 10.1016/J.JINF.2021.12.016.

[22] Suvarna, N. Bappalige, and K. P. Karani, "Enhancing Medical Image Analysis with Convolutional Neural Networks: A Paradigm Shift in Healthcare Diagnostics," pp. 133–139, 2024.

DOI: https://doi.org/10.54216/FPA.210228
Received: April 12, 2025 Revised: June 24, 2025 Accepted: August 20, 2025

[23] Prinzi, C. Militello, Y. Matsuzaka, and R. Yashiro, "The Diagnostic Classification of the Pathological Image Using Computer Vision," *Algorithms*, vol. 18, no. 2, p. 96, Feb. 2025, doi: 10.3390/A18020096.

[24] fatima, R. H. Allami, and M. G. Yousif, "Integrative AI-Driven Strategies for Advancing Precision Medicine in Infectious Diseases and Beyond: A Novel Multidisciplinary Approach," Jul. 2023, Accessed: Aug. 06, 2025. [Online]. Available: http://arxiv.org/abs/2307.15228

[25] Nira and H. Kumar, "Epidemiological Mucormycosis treatment and diagnosis challenges using the adaptive properties of computer vision techniques based approach: a review," *Multimed Tools Appl*, vol. 81, no. 10, pp. 14217–14245, Apr. 2022, doi: 10.1007/S11042-022-12450-W/METRICS.

[26] K. He, X. Zhang, S. Ren, and J. Sun, "Deep residual learning for image recognition," *Proceedings of the IEEE Computer Society Conference on Computer Vision and Pattern Recognition*, vol. 2016-December, pp. 770–778, Dec. 2016, doi: 10.1109/CVPR.2016.90.

[27] D. Mienye, T. G. Swart, G. Obaido, M. Jordan, and P. Ilono, "Deep Convolutional Neural Networks in Medical Image Analysis: A Review," *Information (Switzerland)*, vol. 16, no. 3, Mar. 2025, doi: 10.3390/INFO16030195.

[28] M. Vyas, I. Sehgal, and E. Dannaoui, "Recent Developments in the Diagnosis of Mucormycosis," *Journal of Fungi*, vol. 8, no. 5, p. 457, Apr. 2022, doi: 10.3390/JOF8050457.

[29] D. Dusa and M. R. Gundavarapu, "Smart Framework for Black Fungus Detection using VGG 19 Deep Learning Approach," *8th International Conference on Advanced Computing and Communication Systems, ICACCS 2022*, pp. 1023–1028, 2022, doi: 10.1109/ICACCS54159.2022.9785123.

[30] M. I. Hasan, N. I. Mahbub, and B. Sarkar, "Identification of Black Fungus Diseases Using CNN and Transfer-Learning Approach," *ACM International Conference Proceeding Series*, pp. 118–125, Mar. 2022, doi: 10.1145/3542954.3542972.

[31] S. Karthikeyan, G. Ramkumar, S. Aravindkumar, M. Tamilselvi, S. Ramesh, and A. Ranjith, "A Novel Deep Learning-Based Black Fungus Disease Identification Using Modified Hybrid Learning Methodology," *Contrast Media Mol Imaging*, vol. 2022, 2022, doi: 10.1155/2022/4352730.

[32] P.Sri Lakshmi Durga and M . Kalidas, "BLACK FUNGUS DETECTIONUSING MACHINE LEARNING," *international journal of engineering technology and management sciences*, vol. 6, no. 6, pp. 393–397, Nov. 2022, doi: 10.46647/IJETMS.2022.V06I06.070.

[33] G. S. Annie Grace Vimala, R. Kesavan, E. Manigandan, S. Pushpa Latha, B. V. Kumar, and S. Padmakala, "Black Fungus Infection Detection using AI-based Early Warning System for Patients through Multi-Modal Medical Imaging," *2nd International Conference on Automation, Computing and Renewable Systems, ICACRS 2023 - Proceedings*, pp. 1783–1789, 2023, doi: 10.1109/ICACRS58579.2023.10404938.

[34] P. V. S. Charan and G. Ramkumar, "Mucormycosis Detection using Hybrid Convolutional Neural Network with Support Vector Machine and Compare the performance with Support Vector Machine," *Proceedings of the International Conference on Artificial Intelligence and Knowledge Discovery in Concurrent Engineering, ICECONF 2023*, 2023, doi: 10.1109/ICECONF57129.2023.10083770.

[35] M. Abdul Hameed, M. S. U. Rahman, and A. Banu, "Black Fungus Prediction in Covid Contrived Patients Using Deep Learning," *Intelligent Systems Reference Library*, vol. 231, pp. 309–321, 2023, doi: 10.1007/978-3-031-12419-8_16.

[36] R. Patil *et al.*, "Development of a machine learning model to predict risk of development of COVID-19-associated mucormycosis," *Future Microbiol*, vol. 19, no. 4, pp. 297–305, 2024, doi: 10.2217/FMB-2023-0190.

[37] E. Hassan, A. Saber, E. S. M. El-Kenawy, R. Bhatnagar, and M. Y. Shams, "Early Detection of Black Fungus Using Deep Learning Models for Efficient Medical Diagnosis," *Proceedings of the 2024 International Conference on Emerging Techniques in Computational Intelligence, ICETCI 2024*, pp. 426–431, 2024, doi: 10.1109/ICETCI62771.2024.10704103.

[38] Simonyan and A. Zisserman, "Very Deep Convolutional Networks for Large-Scale Image Recognition," *3rd International Conference on Learning Representations, ICLR 2015 - Conference Track Proceedings*, Sep. 2014, Accessed: Aug. 06, 2025. [Online]. Available: https://arxiv.org/abs/1409.1556v6

DOI: https://doi.org/10.54216/FPA.210228
Received: April 12, 2025 Revised: June 24, 2025 Accepted: August 20, 2025

[39] D. Apostolopoulos, N. D. Papathanasiou, N. Papandrianos, E. Papageorgiou, and D. J. Apostolopoulos, "Innovative Attention-Based Explainable Feature-Fusion VGG19 Network for Characterising Myocardial Perfusion Imaging SPECT Polar Maps in Patients with Suspected Coronary Artery Disease," *Applied Sciences*, vol. 13, no. 15, p. 8839, Jul. 2023, doi: 10.3390/APP13158839.

[40] M. Sandler, A. Howard, M. Zhu, A. Zhmoginov, and L. C. Chen, "MobileNetV2: Inverted Residuals and Linear Bottlenecks," *Proceedings of the IEEE Computer Society Conference on Computer Vision and Pattern Recognition*, pp. 4510–4520, Jan. 2018, doi: 10.1109/CVPR.2018.00474.

[41] O. Iparraguirre-Villanueva, V. Guevara-Ponce, O. R. Paredes, F. Sierra-Liñan, J. Zapata-Paulini, and M. Cabanillas-Carbonell, "Convolutional Neural Networks with Transfer Learning for Pneumonia Detection," *International Journal of Advanced Computer Science and Applications*, vol. 13, no. 9, pp. 544–551, 2022, doi: 10.14569/IJACSA.2022.0130963.

[42] S. I. Saedi and M. Rezaei, "A Modified Xception Deep Learning Model for Automatic Sorting of Olives Based on Ripening Stages," *Inventions*, vol. 9, no. 1, p. 6, Dec. 2023, doi: 10.3390/INVENTIONS9010006.

[43] M. Ennab and H. Mcheick, "Advancing AI Interpretability in Medical Imaging: A Comparative Analysis of Pixel-Level Interpretability and Grad-CAM Models," *Machine Learning and Knowledge Extraction*, vol. 7, no. 1, p. 12, Feb. 2025, doi: 10.3390/MAKE7010012.

DOI: https://doi.org/10.54216/FPA.210228
Received: April 12, 2025 Revised: June 24, 2025 Accepted: August 20, 2025